Journal of Geochemical Exploration 257 (2024) 107367

Contents lists available at ScienceDirect

Journal of Geochemical Exploration

journal homepage: www.elsevier.com/locate/gexplo

Deciphering the ore-forming process of Sb-W deposits through scheelite and stibnite trace element geochemistry

Tianxing Wang [a,b], Shanling Fu [a,*], Neal A. Sullivan [c], Jiangbo Lan [a], Luming Wei [a,b]

[a] State Key Laboratory of Ore Deposit Geochemistry, Institute of Geochemistry, Chinese Academy of Sciences, Guiyang 550081, China
[b] University of Chinese Academy of Sciences, Beijing 100039, China
[c] Vision Geochemistry Ltd., Sudbury, Ontario, Canada

ARTICLE INFO

Keywords:
Scheelite trace element geochemistry
Stibnite trace element geochemistry
Sb-W deposits
Fluid-rock interaction
Ore-forming processes

ABSTRACT

Antimony (Sb) and tungsten (W) and deposits typically form in distinct and unrelated ore-forming environments. However, in rare cases, ore deposits may present combined Sb-W mineralization within a single deposit. These contrasting occurrences introduce uncertainty within the Sb-W ore deposit model, which ultimately guides mineral exploration strategies. Scheelite and stibnite are prevalent ore minerals in Sb-W deposits, making their trace element compositions valuable for enhancing our understanding of the genesis of Sb-W ore systems. In this study, we conducted a systematic investigation of trace element compositions in scheelite and stibnite samples from the Chashan and Zhazixi Sb-W deposits in South China to decipher the primary ore-forming processes. Scheelite from the Sb-W deposits is characterized by low Na, Nb, Ta and Mo contents, and variable Nb/Ta ratios. These results present a remarkably different geochemical signature when compared with granite-related W deposits, indicating that W mineralization in Sb-W deposits was derived from a non-magmatic origin. Moreover, when combining the trace element signature with reported fluid inclusion and isotopic data, it can be concluded that ore-forming fluids of the Chashan and Zhazixi Sb-W deposits were primarily composed of deep-circulating meteoric groundwater. Scheelite from the Chashan deposit presents relatively flat REE patterns with large positive Eu anomalies, whereas the Zhazixi deposit is characterized by bell-shaped REE patterns with weak Eu anomalies. This suggests that the two Sb-W deposits may differ slightly in their source rock composition, which is also supported by the different trace element compositions of stibnite. Stibnite from the Zhazixi deposit is relatively enriched in As, Se and Pb, whereas stibnite from the Chashan deposit contains higher Sn, Zn, Mo, Ag, In and Sr, further indicating that the initial fluids of the two deposits may have undergone different degrees of fluid-rock interaction with their distinctive source rocks. This study demonstrates that the genesis of the Zhazixi and Chashan Sb-W deposits significantly differ when compared to the ore-forming processes that control granite-related W or metamorphic W deposits. Moreover, the formation of these Sb-W deposits appears to share a similar genetic model consistent with low-temperature Sb deposits in South China. In this model, deep-circulating meteoric groundwater infiltrates and leaches Sb and W from fertile source rocks through fluid-rock interaction. Concealed granites may have solely served as a thermal source for the convection and upward migration of ore-forming fluids, while the fertility of source rocks and the intensity of fluid-rock interaction are expected to have played a crucial role in the formation of Sb-W deposits.

1. Introduction

It is well established that W ore deposits are spatially and temporally associated with many important commodities (Mo, Au, Cu, and Sn) are often derived from magmatic-hydrothermal fluids associated with granitoid plutons (Audétat et al., 2000; Webster et al., 2004; Thomas et al., 2005; Hu and Zhou, 2012; Mao et al., 2013; Poulin et al., 2018; Yuan et al., 2018, 2019). In comparison, Sb ore deposits are primarily hosted in (meta-) sedimentary rocks and commonly formed by low-temperature hydrothermal fluids without direct linkage with igneous intrusions (Dill et al., 2008; Gunn, 2014; Hu et al., 2017a; Schulz et al., 2017; Yan et al., 2022; Fu et al., 2023). Due to their distinct metallogenic settings, Sb and W mineralization occurring within a single ore deposit is rarely recognized worldwide and therefore the processes that govern the

* Corresponding author.
E-mail address: fushanling@mail.gyig.ac.cn (S. Fu).

https://doi.org/10.1016/j.gexplo.2023.107367
Received 5 May 2023; Received in revised form 14 November 2023; Accepted 27 November 2023
Available online 2 December 2023

formation of Sb-W deposits are less concerned in previous literature. South China is home to world-class W and Sb deposits, which account for a significant proportion (>50 %) of the world's W and Sb reserves and production (Hu and Zhou, 2012; Mao et al., 2013; Hu et al., 2017a; Yan et al., 2022; Zhao et al., 2022a, 2022b). Among them, a few deposits such as the Zhazixi and Chashan have been recognized as having a unique metal association of Sb-W (Shen et al., 2015; Zeng et al., 2017a). The Sb-W deposits are hosted in (meta-)sedimentary rocks, fault-controlled, characterized by the coexisting of vein-type Sb and W mineralization, and are thought to form via low-temperature hydrothermal fluids (Shen et al., 2015; Zeng et al., 2017a, 2017b; Zhang et al., 2021). However, the processes governing the formation of these Sb-W deposits remain unclear due to the distinct low-grade metamorphism of their host rocks, which distinguishes them from typical orogenic-type deposits. In addition, their lack of clear spatial association with granites sets them apart from granite-related W deposits in South China. Therefore, different viewpoints favoring sedimentary, metamorphic, or magmatic models have proposed in previous studies (He et al., 1996; Nie, 1996; Zhao et al., 2007, 2021; Zeng et al., 2017a; Guo et al., 2018; Cai et al., 2020).

Because scheelite and stibnite are among the primary ore minerals in Sb-W deposits, their trace element composition may record useful information with respect to the origin of ore fluids and source characteristics. As a result, this information may provide new perspectives to understand the ore genesis of Sb-W deposits (Ghaderi et al., 1999; Brugger et al., 2002; Dostal et al., 2009; Song et al., 2014; Fu et al., 2020a, 2022; Silyanov et al., 2022; Stergiou et al., 2022). In recent studies, in-situ laser ablation-inductively coupled plasma-mass spectrometry (LA-ICP-MS) has been successfully adopted in analyzing the scheelite and stibnite trace element geochemistry (Dostal et al., 2009; Song et al., 2014; Guo et al., 2016; Hazarika et al., 2016; Raju et al., 2016; Fu et al., 2020a, 2022; Tang et al., 2022), which has advantages over the digestion ICP-MS approach, particularly in revealing geochemical variations within single mineral grains (i.e., chemical zonation). In this contribution, we systematically investigated the trace element compositions of scheelite and stibnite from the Zhazixi and Chashan Sb-W deposits using LA-ICP-MS to provide new insights into the ore-forming processes of Sb-W deposits.

2. Geological setting and deposit geology

The South China block is composed of the Yangtze Block to the northwest and the Cathaysia Block to the southeast, where both the Zhazixi and Chashan Sb-W deposits are located within the giant Sb metallogenic belt (GSMB) along the southeastern Yangtze block (Fig. 1). The GSMB mainly consists of the traditional Jiangnan orogen belt and Xiangzhong basin to the north and Youjiang basin to the south (Fig. 1; Yan et al., 2022). The basement lithologies of this region mainly consist of Neoproterozoic sequences, including the Lengjiaxi and Banxi groups and their equivalents, which are mainly composed of phyllite, slate, sandstone, siltstone, and schist, with a small amount of tholeiitic lava and volcanoclastic interlayers, while the sedimentary cover comprises Cambrian to Triassic marine sedimentary rocks and Jurassic-Cretaceous and Cenozoic terrigenous sedimentary rocks (Fig. 1; BGMRGX, 1985; BGMRGZ, 2017; BGMRHN, 2017; Hu et al., 2017a, 2017b). Only a small volume of intrusive rocks outcrop in this region, such as sparse granites

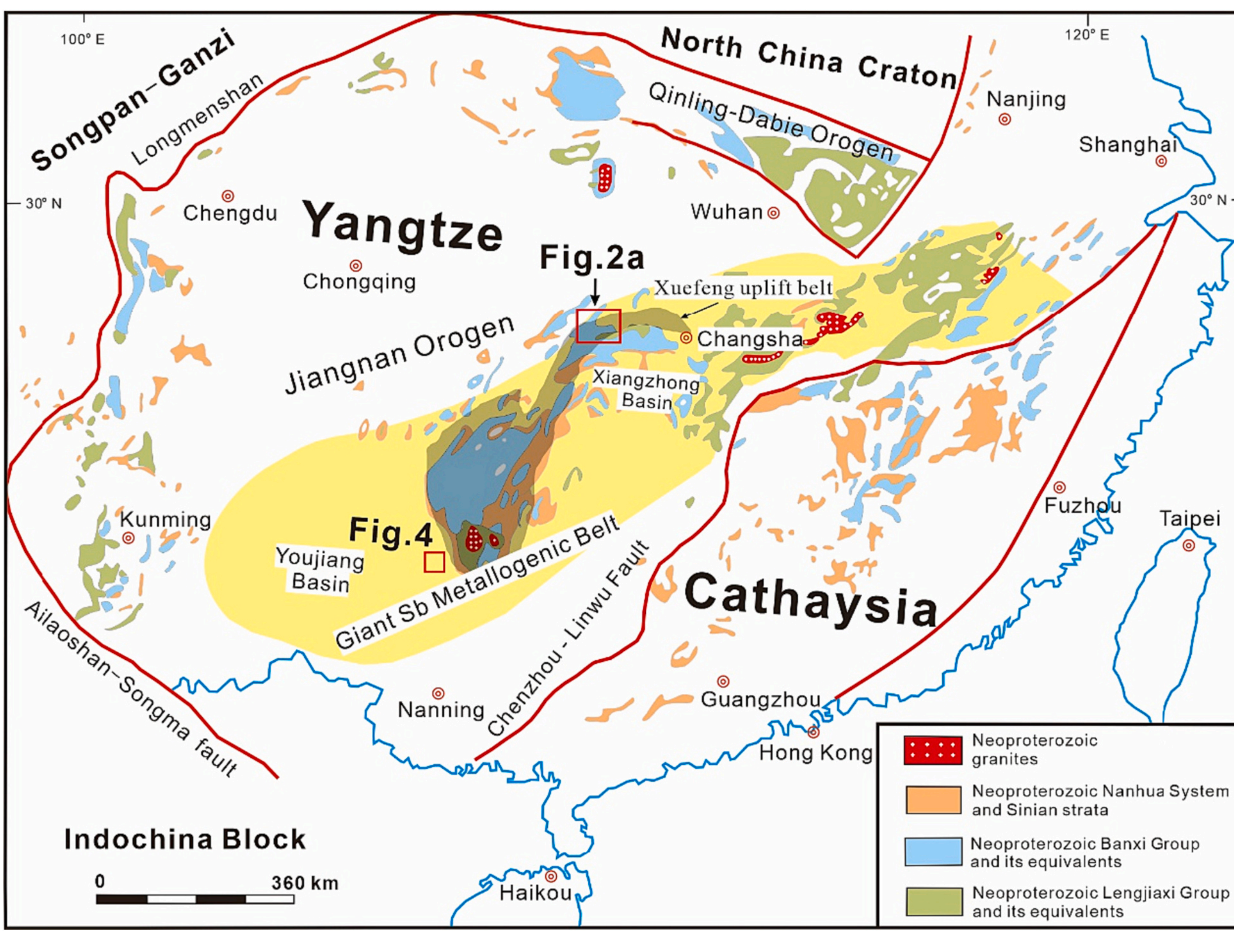

Fig. 1. Simplified geological map of the South China Block showing the locations of the Zhazixi and Chashan Sb-W deposits in South China (Modified after Zhao and Cawood (2012) and Hu et al. (2017b)).

with Neoproterozoic to Early Cretaceous ages in the northeastern part of the Jiangnan orogen belt (Wang et al., 2004; Zhong et al., 2005; Li et al., 2015; Wang et al., 2016; Lu et al., 2017) and minor felsic and mafic dykes with Mesozoic ages in the Xiangzhong and Youjiang basins (Hu and Zhou, 2012; Hu and Peng, 2016; Chen et al., 2016; Pi et al., 2017; Zhu et al., 2017). A large set of Sb, Sb-W, Sb-Au, Sb-Au-W and W deposits are recognized in this region (Hu and Zhou, 2012; Hu et al., 2017a, 2017b; Zhang et al., 2019; Li et al., 2022; Yan et al., 2022; Fu et al., 2023). Among these deposits in the GSMB, Chashan and Zhazixi are the most representative Sb-W deposits.

2.1. Geology of the Zhazixi Sb-W deposit

The Zhazixi deposit is located in the central part of the Xuefengshan uplift and lies in the western segment of the Jiangnan orogen belt (Fig. 1 and Fig. 2a). The Zhazixi deposit contains proven metal reserves of 0.25 million tons of Sb and 13,041 tons of WO_3 with average grades of 9.46 % Sb and 0.82 % WO_3, respectively (Zeng et al., 2017a). Outcropping rocks in the deposit consist mainly of the Wuqiangxi Formation of the Banxi group with Neoproterozoic ages, and to a lesser extent, the Ediacaran and Cambrian (Fig. 2b). Low-grade metasedimentary rocks of the Wuqiangxi Formation are considered to be the most important host rocks, which consist mainly of tuff, tuffaceous sandstone and slate in the upper segment and consist mainly of sandstone, greywacke and quartz sandstone in the lower segment. Structures in the Zhazixi deposit contain interlayer fractures and NW- and NE-trending faults. The former is composed of the interlayer slide interfaces along the boundary between the thick-bedded sandstone and tuffaceous sandstone and their secondary fractures in the thick-bedded sandstone, whereas the latter includes the NW-trending F_3 fault and NE- trending F_1, F_2 and F_4 faults (Fig. 2b; Zeng et al., 2017b). No surface expression of intrusion rocks was observed in the Zhazixi deposit; however, gravity data suggests that there may be concealed granitic plutons deep within the deposit (BGMRHN, 2017).

Sb-W mineralization in the Zhazixi deposit is primarily controlled by interlayer fractures and the NW-trending F_3 fault (Fig. 2c). The W mineralization is strictly confined within interlayer fractures and occurs mainly in the form of veins which are parallel to the host rocks (Peng et al., 2008). The mineral assemblage of W ore veins is composed of mainly of scheelite and quartz with minor stibnite (Fig. 3a–c). While Sb mineralization is predominantly hosted in the NW-trending F_3 fault, the mineral assemblage consists of mainly stibnite and quartz with minor pyrite (Fig. 3d–f). In general, the Sb mineralization converges toward the deep site of the fault but becomes weaker at a distance from the fault. Notably, the interlayer fractures are crosscut by the F_3 fault, indicating that the Sb mineralization may postdate the W mineralization (Lu et al., 2015; Zeng et al., 2017a). Fluid inclusion data suggest that this deposit was generated by low temperature (150–270 °C), low salinity (3.0 %–7.0 wt% NaCl equiv.) and CO_2-bearing ore-forming fluids (Zeng et al., 2017a; Hu and Peng, 2020). Hydrothermal alteration enveloping ore veins includes mainly silicification and local chloritization and carbonatization (Peng et al., 2008; Zeng et al., 2017a).

2.2. Geology of the Chashan Sb-W deposit

The Chashan deposit is located with the Dachang ore-field in the transition between the Jiangnan orogen belt and Youjiang basin (Figs. 1 and 4a) with proven metal reserves of >100,000 tons Sb and >10,000 tons WO_3, and average grades of 1.5 % Sb and 0.36 % WO_3. Multiple types of polymetallic deposits, with variable ore grades, have been found within the Dachang ore-field such as the Tongkeng-Changpo and Gaofeng Sn-Zn-Pb deposits, the Lame Zn-Cu deposit and the Dafulou, Huile, and Kangma Sn-Zn deposits (Fig. 4b), and the Chashan Sb-W deposit is located in the central zone of this ore-field. Strata outcropping in the Chashan deposit comprises Neoproterozoic flysch turbidites, Cambrian sandstone and calcareous shale, Devonian-Triassic flysch sediments, carbonate and minor volcanoclastic rocks (Zhao, 2005; Du et al., 2009; Gao et al., 2010). The Sb-W mineralization in the Chashan deposit is mainly hosted in the Middle Devonian which are mainly composed of muddy limestone interbedded with mudstone, shale and calcareous sandstone (Fan et al., 2004; Cai et al., 2014; Shen et al., 2015; Fig. 5a). Structurally, the Chashan deposit is situated in the western limb of the

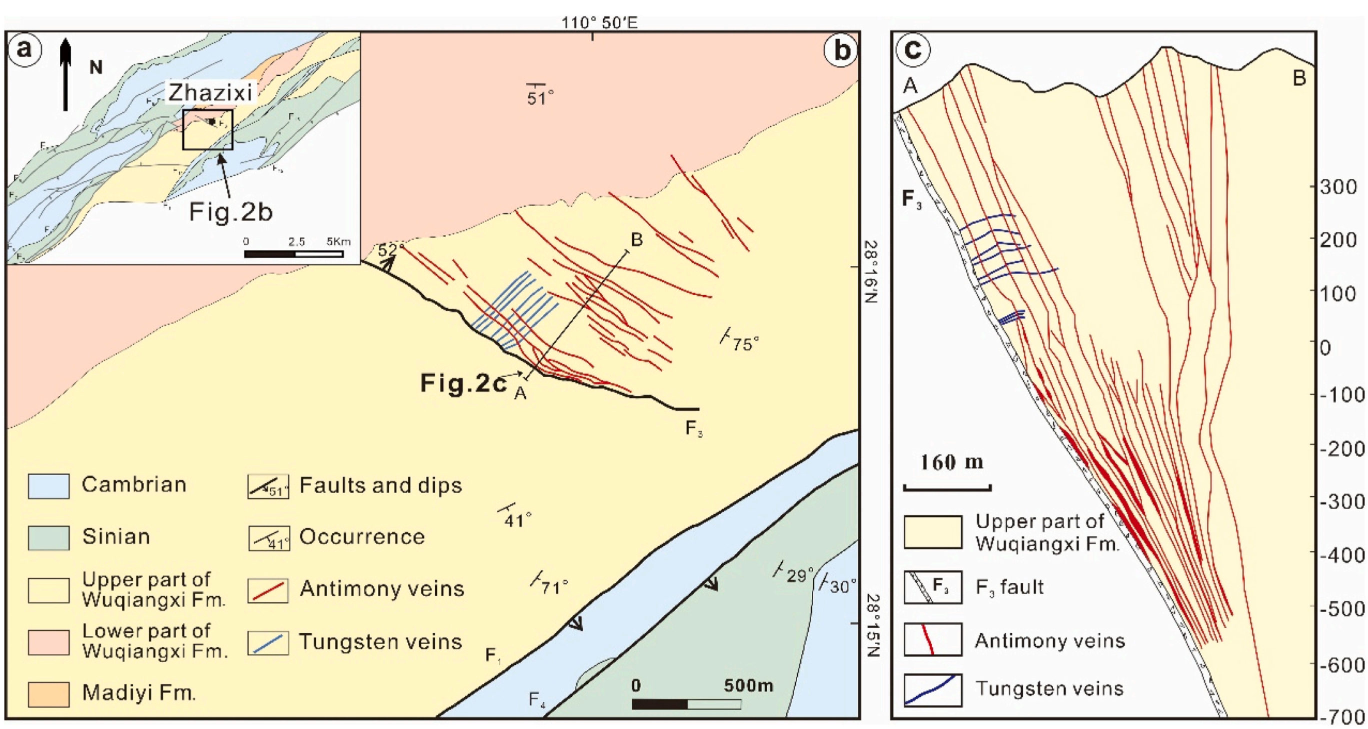

Fig. 2. (a) Geological sketch of Zhazixi Sb ore belt showing the location of the Zhazixi W-Sb deposit, (b) Geological map of the Zhazixi Sb-W deposit and (c) A-B profile showing the mineralization styles of the Zhazixi Sb-W deposit. Fm.-Formation. (Modified after Zeng et al. (2017a)).

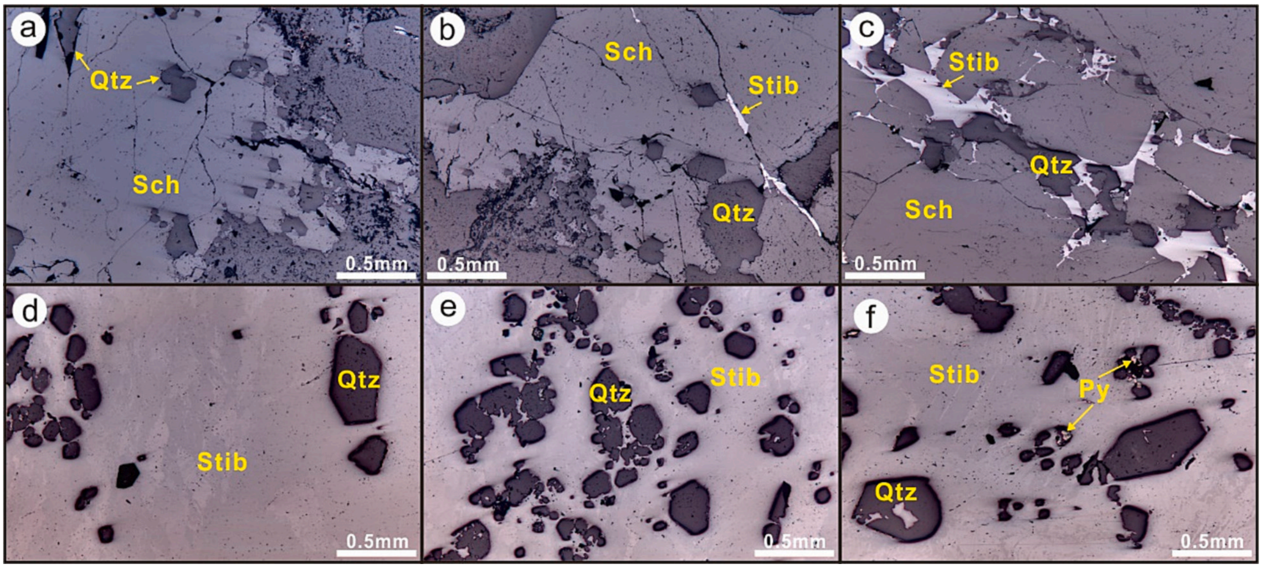

Fig. 3. Reflected light microphotographs of ore samples from the Zhazixi Sb-W deposit. Microphotographs (a)–(c) present W ore, which are mainly composed of scheelite with minor stibnite. Microphotographs (d)–(f) present Sb ore, which are mainly composed of stibnite and quartz with trace amount of pyrite. Qtz-quartz, Stib-stibnite, Sch-scheelite, Py-pyrite.

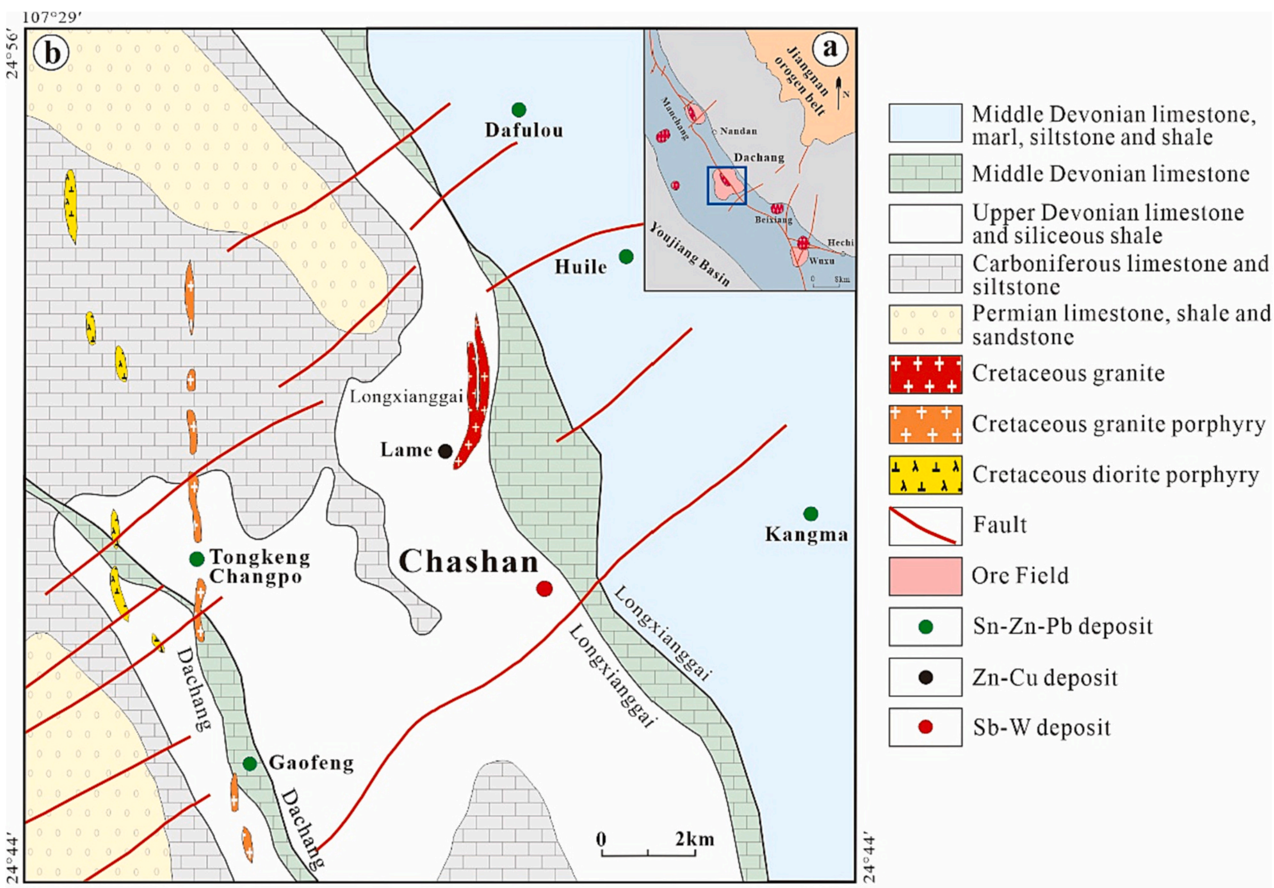

Fig. 4. (a) Geological map showing the occurrence of the Dachang ore district within the transition between the Youjiang Basin and Jiangnan orogen belt (modified after Han et al. (1997)). (b) Geological map of the Dachang Sn-polymetallic ore district, showing the occurrence of the Chashan Sb-W deposit (modified after Jiang et al. (1999) and Zhao et al. (2021)).

Longxianggai anticline where three groups of NE-, NW- and SN-trending faults cut the anticline (Cai et al., 2014; Shen et al., 2015). Intrusive rocks are not observed in the surface expression of the deposit; however, concealed granites were discovered in the drill cores in the northern part of the deposit (Cai et al., 2014).

Unlike the Zhazixi deposit, the Sb-W mineralization in the deposit is

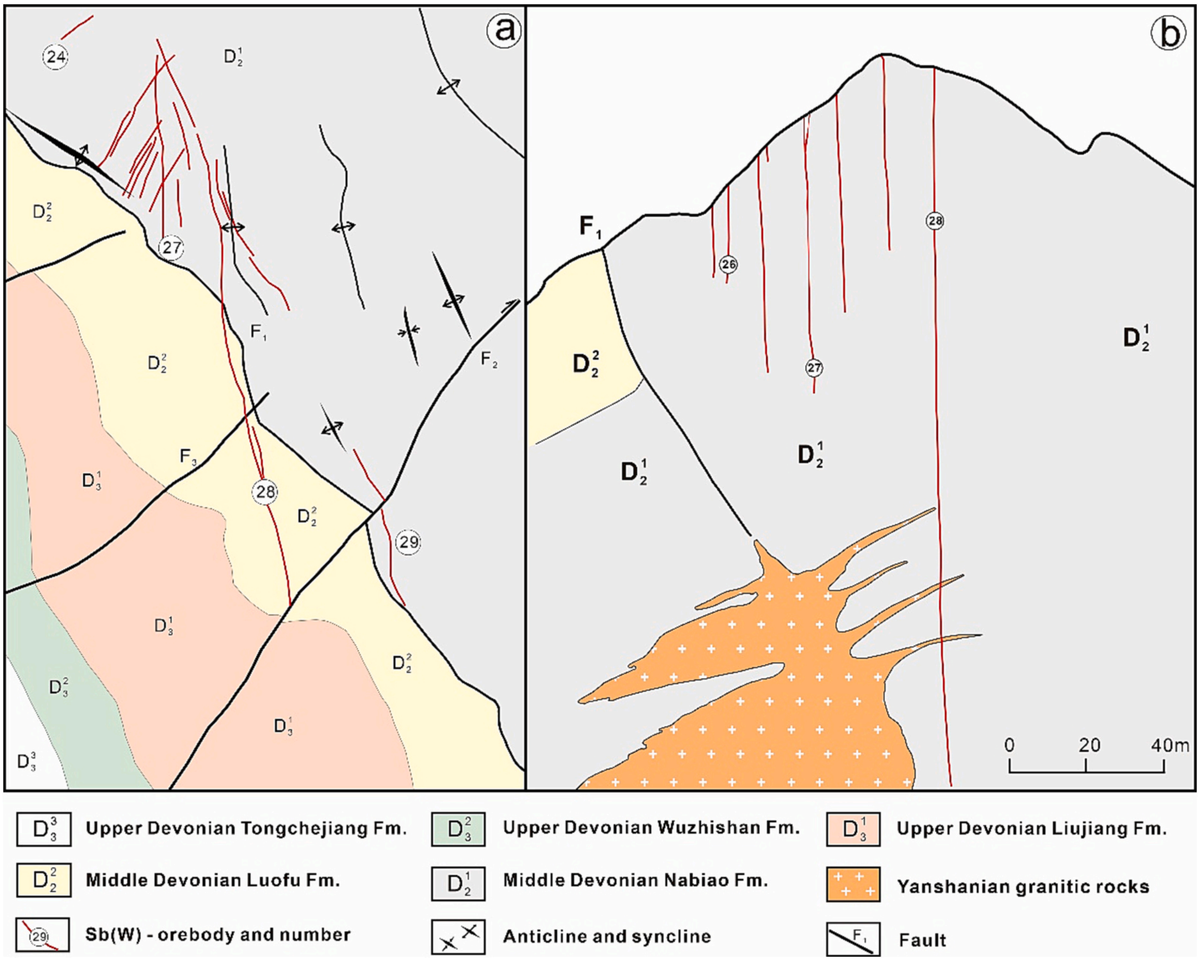

Fig. 5. (a) Geological map of the Zhazixi Sb-W deposit and (b) A representative profile of the Chashan Sb-W deposit showing the occurrence of ore veins and host rocks. Fm.-Formation. (Modified after Liang (2008) and Wang and Wang (2022)).

strictly confined within the NS-trending faults or interlayered fracture zones, and occurs as steeply-dipping veins (Fig. 5b; Nie, 1996; Shen et al., 2015). More than forty ore veins have been found in this deposit. Among them, the ore vein #28 is the largest one and is actively being mined, which extends 3800 m along the strike and >800 m down in dip with a thickness of 0.5–10 m. The average grade of ores is 3.36–3.52 % Sb and 0.28 %–0.51 % WO_3, respectively. The mineral assemblage of ore veins mainly consists of stibnite, berthierite, scheelite, and wolframite as major ore minerals, with gangue minerals including quartz, fluorite, and calcite (Fig. 6). Three mineralization stages have been identified, including i) wolframite-quartz, ii) scheelite-fluorite-calcite, and iii) stibnite-quartz (Cai et al., 2014). Fluid inclusion data suggest that this deposit was generated by low temperature (144–214 °C), relatively high salinity (8.93 %–24.90 wt% NaCl equiv.) ore-forming fluids (Nie, 1998). Hydrothermal alterations related to the Sb-W mineralization in the deposit include silicification, carbonatization, and kaolinization.

3. Samples and analytical methods

All samples were collected from underground exposures in the Zhazixi and Chashan Sb-W deposits. For the Zhazixi deposit, the ZZX-1 and ZZX-2 samples were collected from Sb ore veins with elevations of −115 m and −160 m, respectively, which are composed of mainly stibnite and quartz. ZZX-3 and ZZX-4 samples were collected from W ore veins with elevations of 271 m and 218 m, respectively, which are mainly composed of scheelite and quartz with minor stibnite and pyrite. As the Chashan deposit is tentatively closed with live mining activities, all samples in this deposit were collected from residual ore veins from underground exposures. The analyzed samples (CS-1, CS-2 and CS-5) from this deposit are composed of scheelite, berthierite, stibnite and quartz with minor wolframite.

Trace element analyses of scheelite were conducted at Institute of Geochemistry, Chinese Academy of Sciences (IGCAS), China, using an Agilent 7900 ICP-MS equipped with a GeoLasPro 193 nm ArF excimer laser. The details of analytical processes and reduction of raw data were described in Tang et al. (2022). During the analytical process, helium was applied as a carrier gas which was mixed with Argon via a T-connector before entering the ICP-MS. Spot measurement was performed with the following settings: laser pulse frequency of 6 Hz, spot size of 44 μm, and laser energy of 4.5 J/cm^2. The total analysis time for each spot consists of 20 s measurement of the background with the laser off, and 40 s analysis with the laser on, and a 30 s retention for cell washout. The USGS NIST-610 was employed as external reference material with Ca (measured by EMPA) as the internal standard. NIST-612 (QC) was used as quality control. The detection limits for investigated most elements were below 0.1 ppm and the precision is generally better than 10 %.

Trace element analyses for stibnite were conducted at IGCAS using an Agilent 7700× quadrupole ICP-MS coupled with a New Wave UP213. More details of the analytical processes and reduction of raw data were described in Fu et al. (2020a). Spot measurements were performed with the following settings: laser pulse frequency of 10 Hz, spot size of 60 μm and laser energy of 3.5 J/cm^2. The analysis time for each spot comprises 30 s measurement of background with laser off, and 60 s analysis with

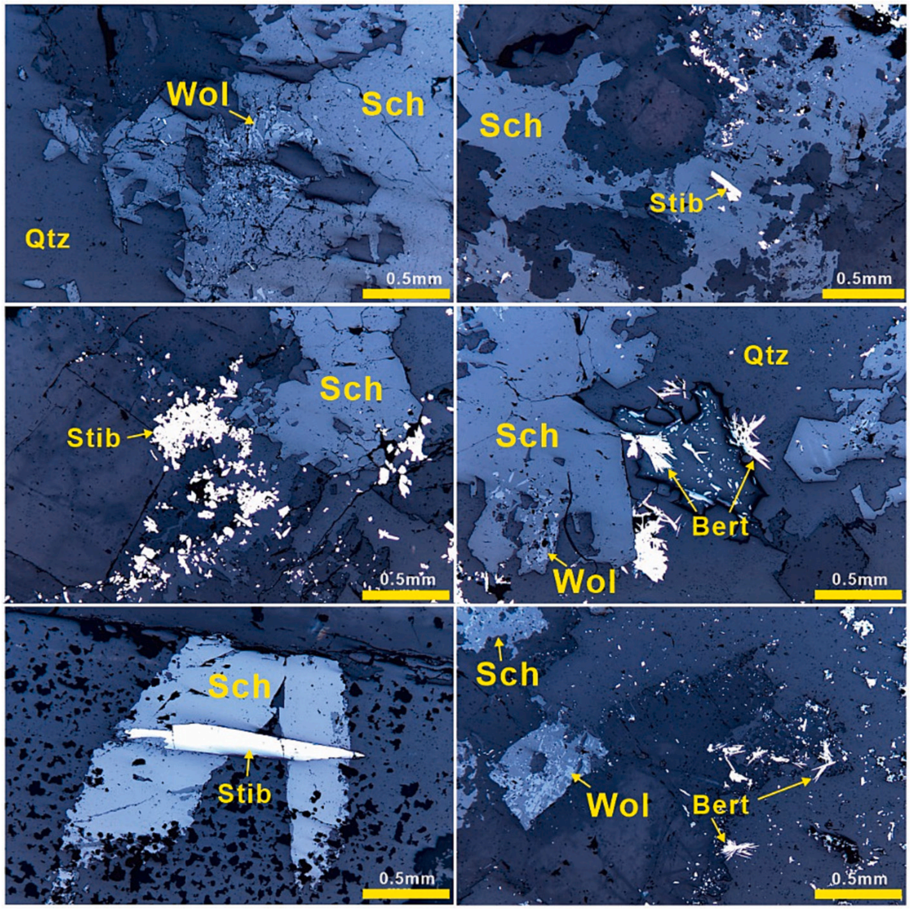

Fig. 6. Reflected light microphotographs of ore samples from the Chashan Sb-W deposit. Ore occurs in the form of veins which are mainly composed of scheelite and stibnite with minor wolframite and berthierite as ore minerals, and quartz as the main gangue mineral. Qtz-quartz, Stib-stibnite, Sch-scheelite, Wol-wolframite, Bert-berthierite.

laser on, and 30 s retention for cell washout. MASS-1 was measured as internal standard, and UAGS NIST SRM 610 and 612 were additionally measured to monitor possible instrumental drift. The accuracy for most elements is better than 10 % with variations in spot size.

4. Results

4.1. Trace element composition of scheelite

A total of 114 LA-ICP-MS trace element analyses were performed on two scheelite samples from the Zhazixi deposit and three scheelite samples from the Chashan deposit. The trace element compositions of scheelite are given in Electronic Supplementary Table S1. In general, scheelite has relatively low abundances of Na, Nb, Mo, Y, Cu, Pb, Sn, Ge

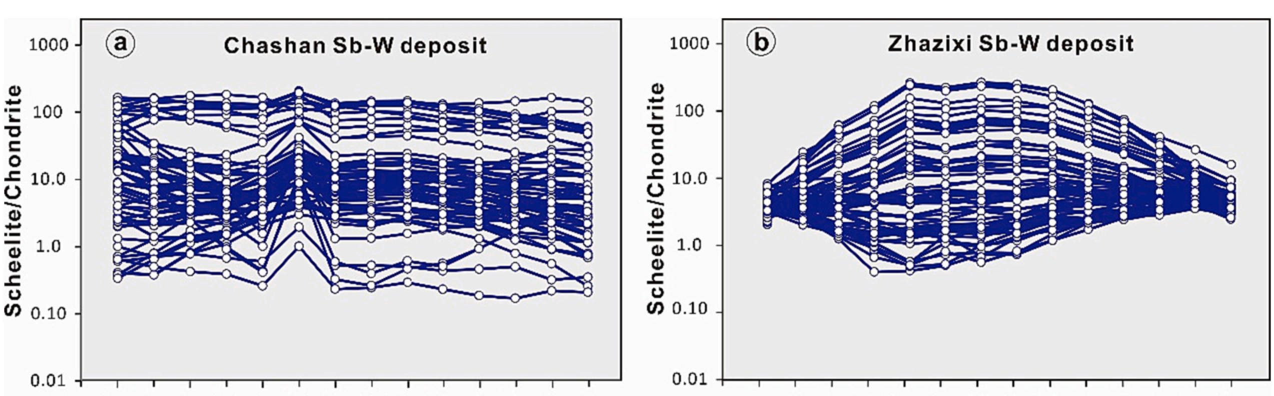

Fig. 7. Chondrite-normalized REE patterns of the scheelite from the (a) Chashan Sb-W deposit and (b) Zhazixi Sb-W deposit. The normalization values are sourced from Sun and McDonough (1989). The REE of scheelite from the Chashan deposit is featured by a relatively flat pattern with large positive Eu anomalies whereas scheelite from the Zhazixi deposit exhibits a bell-shaped pattern with weak positive Eu anomalies.

and Rb with contents ranging between 0.01 and 100 ppm. Scheelite from the Zhazixi deposit has relatively high Sr and Sn, but lower Sb contents compared to samples from the Chashan deposit. Notably, the Sr content of scheelite from the Zhazixi deposit (average 3308 ppm) is approximately one order magnitude greater than that of scheelite from the Chashan deposit (average 694 ppm). In addition, the REE contents of scheelite from the Chashan deposit are relatively high and display relatively flat chondrite-normalized REE patterns with significant positive Eu anomalies (Fig. 7a) compared to those of scheelite from the Zhazixi deposit, which present bell-shaped REE patterns without pronounced Eu anomalies (Fig. 7b).

4.2. Trace element composition of stibnite

A total of forty-two LA-ICP-MS analyses were performed on four stibnite samples from the Zhazixi and Chashan Sb-W deposits. The trace element compositions of stibnites are presented in the Electronic Supplementary Table S2. Arsenic, Cu, Pb, and Se are the most abundant trace elements in the stibnite from both Sb-W deposits with contents ranging from tens to hundreds of ppm. However, stibnite from the Zhazixi deposit is relatively enriched in As and Se with contents of typically >300 ppm, whereas the stibnite from the Chashan deposit is relatively enriched in Sn, Zn, Ag, and In with contents of several to hundreds of ppm (Table S2; Fig. 8).

5. Discussion

5.1. Scheelite trace element geochemistry constraints on the origin of ore fluids

The trace element compositions of scheelite are generally controlled by redox state, pressure-temperature conditions, fluid compositions, and host rock types (Brugger et al., 2000, 2008; Dostal et al., 2009; Song et al., 2014; Guo et al., 2016; Sun and Chen, 2017) and therefore may serve as an indicator to understand the characteristics and source of ore fluids. For example, Mo can only be incorporated into the scheelite crystal structure under oxidizing conditions through coupled substitution of $Mo^{6+} \leftrightarrow W^{6+}$ (Ghaderi et al., 1999; Rempel et al., 2009; Song et al., 2014) such that the Mo contents of scheelite can act as a robust proxy for the redox state of ore fluids. Moreover, because Eu^{2+} can more readily replace the Ca site (compared to Eu^{3+}), positive Eu anomalies are expected for scheelite formed by reduced fluids whereas oxidizing fluids often produce negative Eu anomalies in scheelite (Ghaderi et al., 1999; Xiong et al., 2006; Song et al., 2014). Therefore, Eu anomalies in scheelite can also be used to estimate redox conditions of ore fluids (Ghaderi et al., 1999; Brugger et al., 2000, 2008; Xiong et al., 2006; Song et al., 2014; Sun and Chen, 2017; Zhao et al., 2018). In this study, results from trace element geochemistry suggest that scheelite from the Chashan and Zhazixi Sb-W deposits exhibits extremely low Mo contents and large positive Eu anomalies (Fig. 9), and therefore, it may be inferred that ore fluids of the Chashan and Zhazixi Sb-W deposits were dominated by reduced fluids, which is in contrast with fluids in magmatic-related settings that are more oxidized and enriched in Mo. In addition, scheelite from Chashan and Zhazixi Sb-W deposits is featured by low Na, Nb, Ta, and Mo but high Sr contents. This feature distinguishes it

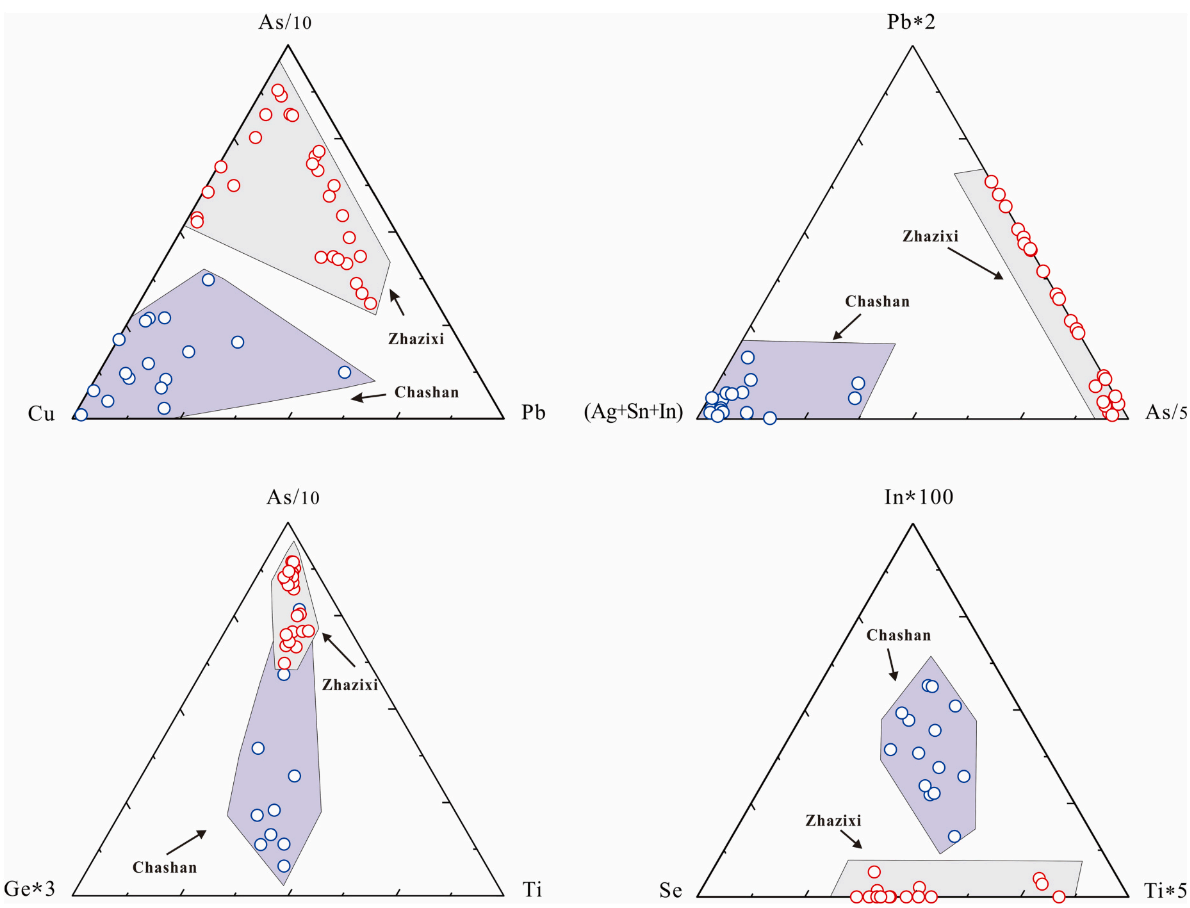

Fig. 8. Ternary plots of trace element compositions in stibnite from the Zhazixi and Chashan Sb-W deposits. Stibnite from the Zhazixi deposit is relatively enriched in As, Cu, and Pb, whereas the Chashan deposit is more enriched in Sn, Zn, Mo, Ag and In, indicating that their source rocks may contain different compositions.

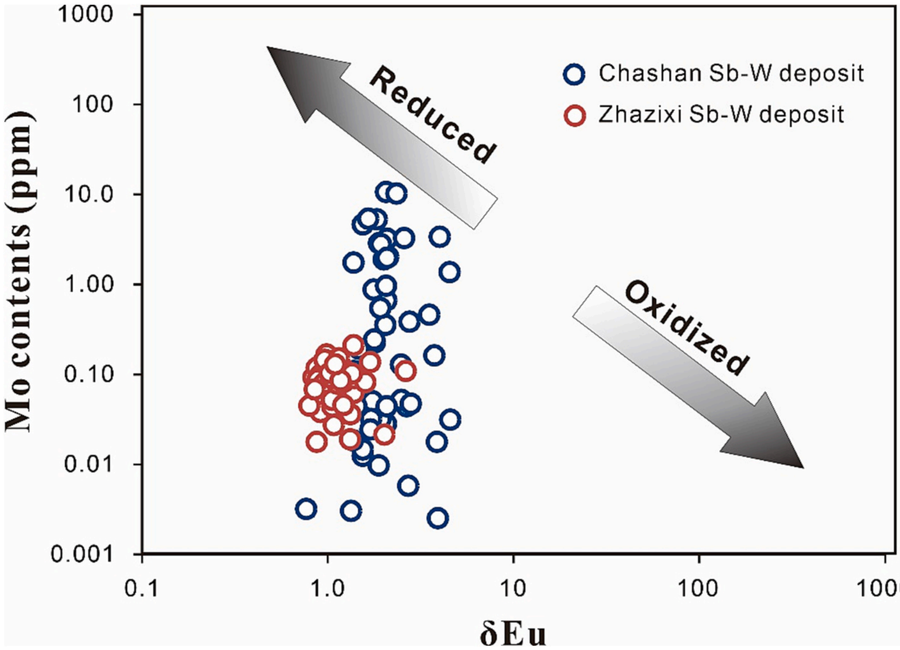

Fig. 9. Plot of Mo vs. δEu in scheelite from the Zhazixi and Chashan Sb-W deposits. The extremely low Mo contents and large positive δEu values suggest that these Sb-W deposits were likely generated from non-magmatic reduced fluids.

significantly from scheelite formed by magmatic-hydrothermal fluids, which typically exhibit enrichment in Na, Nb, Ta, and Mo, depletion in Sr, and negative Eu anomalies (Dolejs and Wagner, 2008; Li et al., 2018a, 2019b; Poulin et al., 2018; Fu et al., 2021). This indicates further that the ore fluids of these Sb-W deposits were of a non-magmatic origin. Studies suggest that the latest peak metamorphism of sedimentary rocks in South China occurred at 460–400 Ma (Faure et al., 2009), much earlier than the mineralization ages of the Chashan (~90 Ma; Guo et al., 2018) and Zhazixi Sb-W deposits (227 Ma; Wang et al., 2012), suggesting that the fluids contributing to ore-forming processes are unlikely of metamorphic origin. The REE patterns of scheelite from the Sb-W deposits are distinct from those of metasedimentary rocks in South China whose REE patterns are typically known as right-dip type REE patterns with negative Eu anomalies (Fan et al., 2004; Li et al., 2019a; Wang et al., 2019), therefore indicating that ore fluids of the Sb-W deposits were not directly generated from their host rocks.

Fluid inclusion data suggests that the ore fluids of the Chashan and Zhazixi Sb-W deposits are characterized by low temperatures with low H-O isotope values (δD = −80 ‰ ~ −58 ‰, $\delta^{18}O$ = −3.8 ‰ ~ −2.4 ‰ for the Chashan deposit and δD = −61 ‰ ~ −65 ‰, $\delta^{18}O_{H2O}$ = −6 ‰ ~ −8 ‰ for the Zhazixi deposit), suggesting that their ore fluids may have been dominated by deep-circulating meteoric groundwater (He et al., 1996; Nie, 1998). However, it should be noted that meteoric groundwater normally contains very low REE contents, and thus deep-convecting meteoric groundwater cannot account for the sole origin of the ore fluids that generated the REE signature in the Sb-W deposits. Therefore, it is reasonable to infer that the REE characteristics of ore fluids may have resulted from fluid mixing or extensive fluid-rock interaction. The two elements Y and Ho share parallel geochemical behavior due to their similar ionic radii and ionic charge (Bau and Dulski, 1995), in that they retain their corresponding chondritic ratio in a single fluid source but become sensitive to fractionation when the mixing of different origin fluids occurs (Bau and Möller, 1992; Irber, 1999; Liu et al., 2019). Results from this study show a strong positive correlation between Y and Ho in scheelite (Fig. 10a), suggesting that fluid mixing may have been insignificant for the ore fluids of the

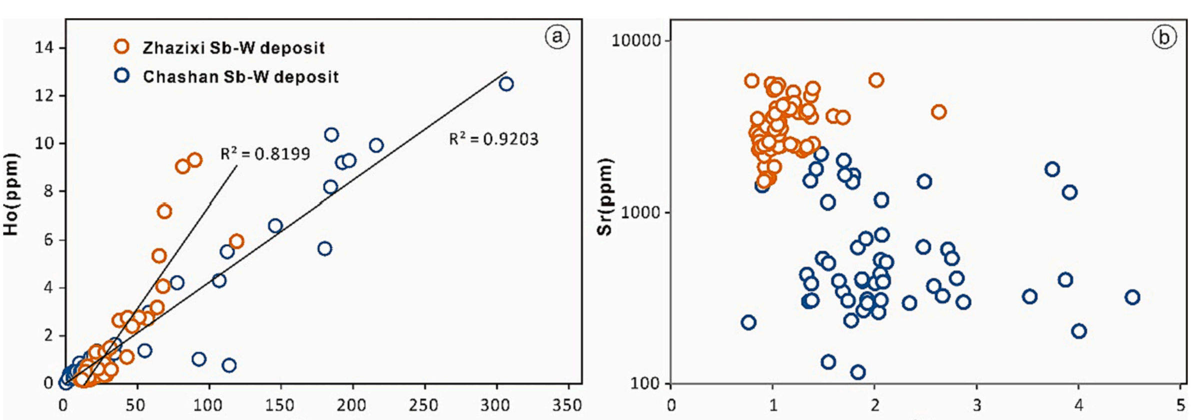

Fig. 10. Plots of (a) Y vs. Ho and (b) δEu vs. Sr contents in scheelite from the Zhazixi and Chashan Sb-W deposits. The strong positive correlation between Y and Ho suggests that fluid mixing was insignificant during the ore fluid evolution of the Sb-W deposits considering Y and Ho retain their corresponding chondritic ratio in a single-stage fluid source but vary when the mixing of different origin fluids occurs (Bau and Möller, 1992; Irber, 1999).

Chashan and Zhazixi Sb-W deposits. In contrast, Sr may be used as a proxy to assess the level of fluid-rock interaction (Barker et al., 2009; Satish-Kumar et al., 2010; Beaudoin and Chiaradia, 2016). Because Sr preferentially partitions into fluids during fluid-rock interaction, higher contents of Sr indicate higher intensity of fluid-rock interaction. The results from Fig. 10b present high and variable Sr contents in scheelite from the Chashan and Zhazixi Sb-W deposits, therefore suggesting that their ore fluids may have been interacted with Sr-rich rocks (Peng et al., 2008; Shen et al., 2015; Zhang et al., 2021). While it seems evident that both deposits show some level of fluid-rock interaction, it should be noted that the two deposits show different set of REE patterns in scheelite (Fig. 7), indicating that their initial fluids may have interacted with source (and/or host) rocks of different compositions during the migration of ore fluids. The contrasting and large variations of Eu anomalies (Fig. 9; δEu = 0.8–4.6 in the Chashan deposit and 0.8–2.6 in the Zhazixi deposit) also provide support that the initial fluids of the two deposits may have interacted with different compositions of source rocks which modified their compositions during fluid migration. Overall, the trace element geochemistry of scheelite, paired with isotopic data, lends support to a model that suggests the ore fluids from the Chashan and Zhazixi Sb-W deposits likely originated from deep-convecting meteoric groundwater that was modified by extensive fluid-rock interaction with different source or/and host rocks, rather than by magmatic or metamorphic processes.

5.2. *Trace element geochemistry of stibnite constraints on the metal source*

Stibnite is the most common Sb-bearing mineral phases observed in various types of Sb deposits and thus trace element chemistry of stibnite can be used to identify the metal source of hydrothermal Sb deposits (Fu et al., 2020a, 2022; Silyanov et al., 2022; Stergiou et al., 2022). Stibnite has a simple configuration of Sb-S bonds with limited void space, in such that only a few trace elements can be incorporated into its crystal lattice. The elevated contents of As, Cu and Pb in stibnite from the Chashan and Zhazixi Sb-W deposits are likely controlled by the coupled substitution of $2Sb^{3+} \leftrightarrow Cu^{+} + Pb^{2+} + As^{3+}$ (Fu et al., 2020a) while the measurable Se content is expected to originate by the substitution of $S^{2+} \leftrightarrow Se^{2+}$ in the crystal lattice (Kyono et al., 2015). Notably, however, stibnites from the two deposits show apparent differences in trace element compositions, indicating their source rocks might be of different composition (Fu et al., 2020a; Silyanov et al., 2022; Stergiou et al., 2022). For instance, stibnite from the Chashan deposit contains higher Sn, Ag, In, and Zn contents compared to the Zhazixi deposit (Fig. 8), indicating that the source rocks of the Chashan deposit may have been relatively enriched in these metals. This inference is further supported by multiple occurrences of Sn-Zn-Ag (-In) polymetallic deposits in the adjacent region of the Chashan Sb-W deposit (Fan et al., 2004; Guo et al., 2018; Zhang et al., 2018; Zhao et al., 2021). Therefore, it may be concluded that fertile rocks deeply located in the Chashan region (Shen et al., 2015) may have served as the metal source for Sb-W mineralization in the Chashan deposit and also as a potential source for Sn, Ag, Zn, and In for polymetallic deposits in the region. Moreover, the Devonian host rocks of the Chashan deposit that are enriched in W and Sb may have also contributed to the metal budget of the deposit during fluid-rock interaction (Nie, 1996).

In comparison, stibnite from the Zhazixi deposit is more enriched in As, Se and Pb and compositions are similar to the sediment-hosted Xikuangshan, Woxi and Banxi Sb deposits adjacent to Zhazixi (Fu et al., 2020a, 2022), possibly indicating that they may have shared a common metal source. Previous studies suggested that sediment-hosted Sb deposits in central Hunan were likely generated from deep-convecting meteoric groundwater interaction with Proterozoic metamorphic rocks (fluid-rock interaction) which led to the extraction of Sb and W metals (Peng et al., 2010; Liang et al., 2014; Zhu and Peng, 2015; Li et al., 2018a, 2018b, 2019a, 2022; Fu et al., 2020c, 2023; Long et al., 2022). Similarly, it can be inferred that the Sb-W metals of the Zhazixi deposit may also have been primarily sourced from the fertile Proterozoic metamorphic rocks. The coupled enrichment of Sb and W was also observed in the basement metasedimentary rocks of the Zhazixi deposit and adjacent districts (Lu et al., 2001; author's unpublished data), providing additional evidence that the Sb-W metals were likely sourced from these fertile metasedimentary rocks of the Zhazixi deposit.

Considering the variability in stibnite trace element compositions between the Chashan and Zhazixi Sb-W deposits, it is anticipated that the source rocks differ in their geochemical compositions. For example, the source rocks of the Zhazixi deposit were relatively enriched in As, Sb and W and thus resulted in the formation of large-scale Sb, W and even Au deposits. Whereas the source rocks of the Chashan deposit were more enriched in Sn, Zn, In and Ag in addition to Sb and W, in such that a set of Sb-W deposits and Sn-Zn-Pb-Ag-In polymetallic deposits were formed in the Chashan and adjacent districts. These implications may be helpful to guide future prospecting and exploration of Sb-W polymetallic deposits in the Chashan and Zhazixi districts.

5.3. *Genetic model for the Sb-W deposits*

Most W polymetallic deposits observed around the world commonly have a genetic link with granites, where granitic magmas are thought to either directly supply fluids and metals, or they serve as a heat source thereby circulating fluids and leaching of metals from their source rocks (Linnen and Williams-Jones, 1995; Audétat et al., 2000; Webster et al., 2004; Thomas et al., 2005; Song et al., 2014; Sun et al., 2019). Geophysical data and drilling results suggest that there might be concealed granitic rocks in the Zhazixi and Chashan districts (Shen et al., 2015; BGMRHN, 2017; Zeng et al., 2017a Guo et al., 2018; Wang et al., 2019), indicating a potential genetic link between the Sb-W deposits and proximal granitic rocks. However, trace element compositions in scheelite from the Chashan and Zhazixi deposits are distinct from trace element signatures of scheelite with a magmatic origin, indicating that these deposits were unlikely formed by the commonly accepted model, in which the ore fluids and metals are exsolved exclusively from the granite plutons (Audétat et al., 2000; Webster et al., 2004; Thomas et al., 2005; Song et al., 2014; Harlaux et al., 2018; Sun et al., 2019). In addition, the scheelite REE signatures from the Chashan and Zhazixi Sb-W deposits are characterized by relatively flat to bell-shaped REE patterns showing large positive Eu anomalies. This suggests that they unlikely inherited their REE signatures from the Mesozoic granites in South China, which are characterized by the typical "right-dip type" showing negative Eu anomalies (Shi et al., 2007; Liang, 2008; Sun et al., 2019). Moreover, experimental results determined that the fluid-melt and mineral-melt partition coefficients of Sb are relatively low (~1.0; Audétat et al., 2000; Audétat and Pettke, 2003; Simons et al., 2017; Fu et al., 2020b), in such that Sb would not be preferentially enriched in the evolved magmatic fluids. As a result, granitic magmas may have only served as a thermal source by driving the transportation of ore fluids, without any contribution to the budget of metal of the Chashan and Zhazixi Sb-W deposits.

Studies on the behavior of Sb and W in metamorphic terranes suggest that Sb and W may be mobilized during prograde metamorphism and enriched in the metamorphic fluids between greenschist and amphibolite facies (Pitcairn et al., 2006, 2010). However, the Neoproterozoic metasedimentary rocks in South China were generally subject to sub-greenschist or lower grades of metamorphism which is considered too weak to significantly promote the mobility of Sb and W (Pitcairn et al., 2006, 2015; Phillips and Powell, 2010). More importantly, the peak metamorphism of metamorphic rocks in South China was determined to be significantly older than the ages of the Sb-W deposits (Faure et al., 2009; Yan et al., 2022), indicating that they were less likely generated through regional-scale metamorphism. In the LREE-MREE-HREE ternary diagram (Fig. 11), the REE compositions of scheelite in the Chashan and Zhazixi Sb-W deposits are remarkably different from those

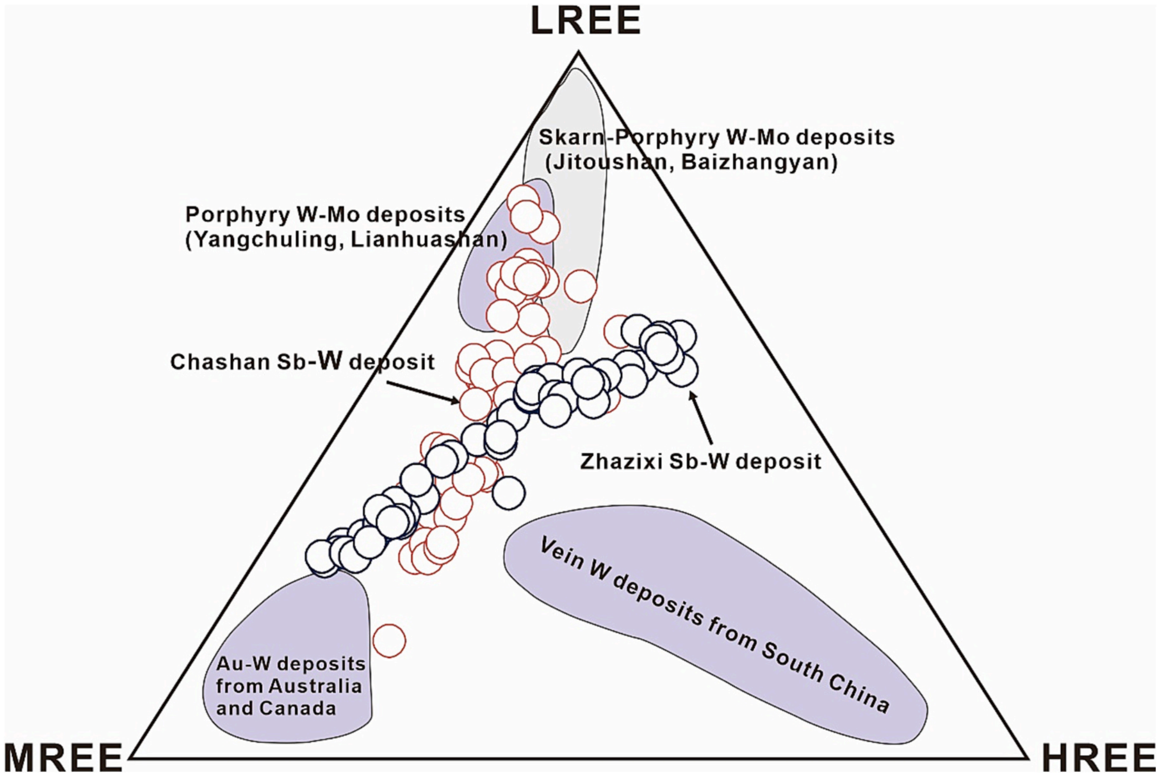

Fig. 11. Ternary LREE-MREE-HREE diagram of scheelite from the Zhazixi and Chashan Sb-W deposits. The REE data of scheelite from vein-type Au-W, vein-type W, and porphyry-type W-Mo deposits were sourced from Henderson (1985), Zhang et al. (1990), Raimbault et al. (1993), Sylvester and Ghaderi (1997), Ghaderi et al. (1999), Brugger et al. (2000, 2002, 2008), Dostal et al. (2009), and Peng et al. (2010).

of granite-related vein-type W deposits, skarn-porphyry W-Mo deposits in South China, and metamorphic Au-W deposits in Australia. Therefore, it is reasonable to conclude that the Chashan and Zhazixi Sb-W deposits were unlikely to have been formed by a magmatic or metamorphic model.

Alternatively, experiments have demonstrated that Sb and W are strongly mobile in aqueous solutions relevant to hydrothermal environments, even at low temperatures (Lassner and Schubert, 1999; Zotov et al., 2003; Dermatas et al., 2004) and thus it is possible that considerable contents of Sb and W metal may be scavenged from fertile rocks during fluid-rock interaction. For example, leaching experiments suggested that low-T (<300 °C) fluids flowing through Sb-rich metasedimentary rocks are able to leach about 40–70 % of the Sb content (Ewers, 1977; Ma et al., 2002). Considering the strong mobility of Sb and W in experiments, remobilization of Sb and W in fertile rocks during fluid-rock interaction may be an effective ore-forming process for Sb-W deposits hosted in sedimentary rocks. Therefore, the formation of Sb-W deposits can be elucidated by a genetic model (Fig. 12) wherein deep-convecting meteoric groundwater infiltrates and leaches Sb and W from fertile Proterozoic basements and host rocks to generate ore fluids, in such that concealed granites may have solely acted as a thermal source for the convection and upward migration of ore-forming fluids, while the fertility of source rocks and the intensity of fluid-rock interaction are crucial for the formation of Sb-W deposits hosted in sedimentary rocks, distinguishing them from granite-related and metamorphic W deposits.

6. Conclusions

Scheelite and stibnite trace element compositions suggest that the ore-forming processes governing the generation of the Chashan and Zhazixi Sb-W deposits differ from vein-type W polymetallic deposits, which commonly present a genetic association with granitic magmas. Moreover, the Sb-W deposits were also determined to be distinct from traditional Au-W deposits, which tend to derive from metamorphic processes. Alternatively, it is plausible that the Sb-W deposits were formed through a remobilization process involving fertile Proterozoic basements and host rocks. This process entails the interaction between deep-convecting meteoric groundwater and fertile source rocks, resulting in the scavenging of Sb and W into ore fluids and eventually leading to the precipitation of stibnite and scheelite in the Chashan and Zhazixi deposits. Deep-seated granitic intrusions are suggested to have served only as a thermal source by driving fluid-rock interaction and promoting Sb and W scavenging. Notably, the intensity of fluid-rock interaction and the fertility of source rocks likely played a vital role in determining the formation of Sb-W deposits. This study also highlights that the trace element geochemistry of primary ore minerals is a valuable approach for deciphering the ore-forming processes of Sb-W deposits with a relatively simple mineral assemblage.

CRediT authorship contribution statement

All the authors listed in the manuscript have read this paper and approved its final submission.

Tianxing Wang: Field investigations, Conceptualization, Methodology, Data Curation Writing-Original Draft, Writing – Review & Editing
Shanling Fu: Field investigations, Conceptualization, Supervision, Funding acquisition, Writing - Review & Editing
Neal A. Sullivan: Conceptualization, Writing – Review & Editing
Jiangbo Lan: Field investigations, Preparation
Luming Wei: Field investigations, Methodology

Declaration of competing interest

The authors declare that they have no known competing financial interests or personal relationships that could have appeared to influence

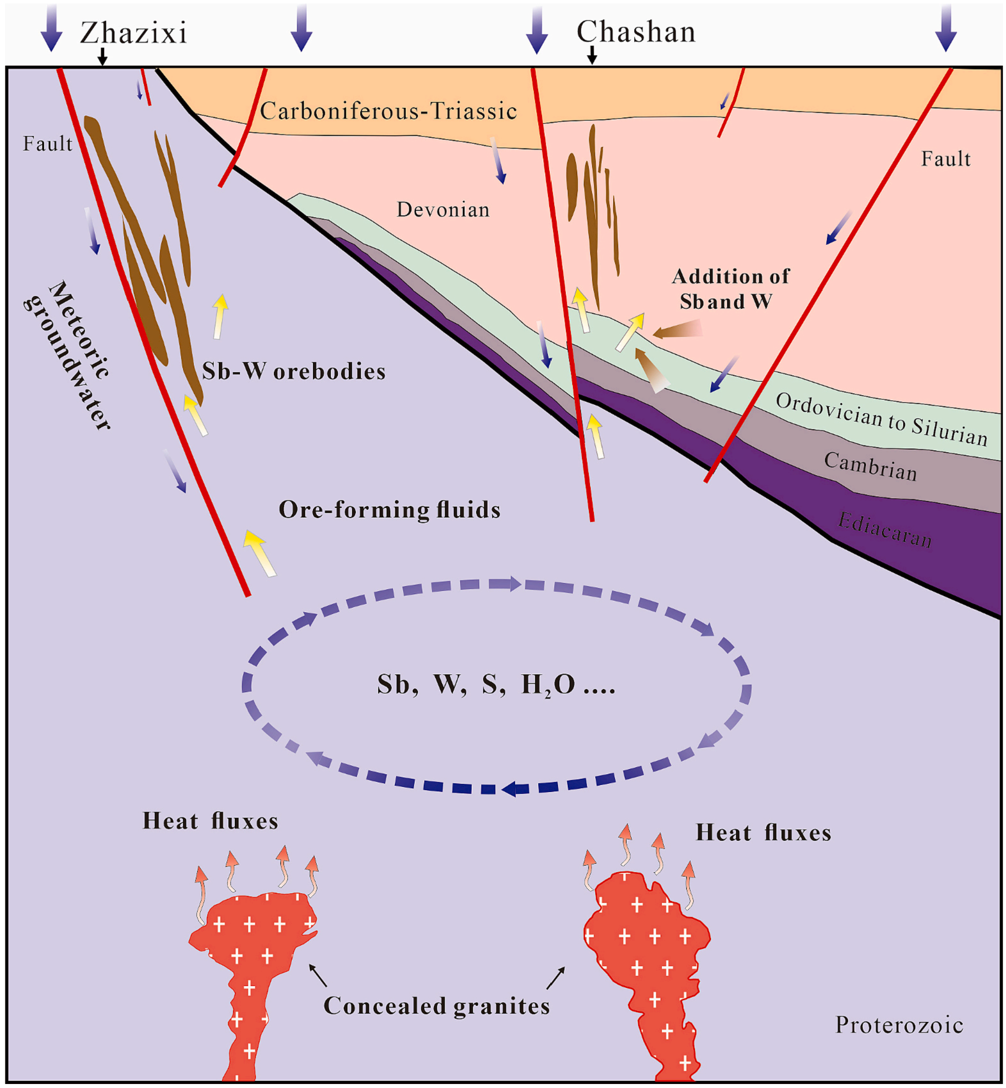

Fig. 12. Schematic diagram for the formation of the Zhazixi and Chashan Sb-W deposits in South China.

the work reported in this paper.

Data availability

No data was used for the research described in the article.

Acknowledgements

This study is jointly funded by the National Key Research and Development Program of China (2023YFC2906801), National Natural Science Foundation of China (42272102 and 92162323) and the Field Forefront Project of the State Key Laboratory of Ore Deposit Geochemistry, IGCAS (202102). We would like to thank Dr. Yanwen Tang and Dr. Zhihui Dai for their assistance with scheelite and stibnite trace element analysis using LA-ICP-MS at IGCAS.

Appendix A. Supplementary data

Supplementary data to this article can be found online at https://doi.org/10.1016/j.gexplo.2023.107367.

References

Audétat, A., Pettke, T., 2003. The magmatic-hydrothermal evolution of two barren granites: a melt and fluid inclusion study of the Rito del Medio and Canada Pinabete plutons in northern New Mexica (USA). Geochim. Cosmochim. Acta 67, 97–121.

Audétat, A., Günthe, D., Heinrich, C.A., 2000. Magmatic-hydrothermal evolution in a fractionating granite: a microchemical study of the Sn-W-F-mineralized Mole Granite (Australia). Geochim. Cosmochim. Acta 64, 3373–3393.

Barker, S.L.L., Bennett, V.C., Cox, S.F., Norman, M.D., Gagan, M.K., 2009. Sm–Nd, Sr, C and O isotopesystematics in hydrothermal calcite-fluorite veins: implications for fluid-rock reaction and geochronology. Chem. Geol. 268, 58–66.

Bau, M., Dulski, P., 1995. Comparative study of yttrium and rare-earth element behaviours in fluorine-rich hydrothermal fluids. Contrib. Mineral. Petrol. 119, 213–223.

Bau, M., Möller, P., 1992. Rare earth element fractionation in metamorphogenic hydrothermal calcite, magnesite and siderite. Mineral. Petrol. 45, 231–246.

Beaudoin, G., Chiaradia, M., 2016. Fluid mixing in orogenic gold deposits: evidence from the H-O-Sr isotope composition of the Val-d'Or vein field (Abitibi, Canada). Chem. Geol. 437, 7–18.

BGMRGX (Bureau of Geology and Mineral Resources of Guangxi Province), 1985. Regional Geology of Guangxi Autonomous Region. Geological Publishing House, Beijing, pp. 1–853 (in Chinese with English Abstract).

BGMRHN (Bureau of Geology and Mineral Resources of Hunan Province), 2017. Regional Geology of Hunan Province. Geological Publishing House, Beijing, pp. 1–1268.

BGMRGZ (Bureau of Geology and Mineral Resources of Guizhou Province), 2017. Regional Geology of Guizhou Province. Geological Publishing House, Beijing, p. 1153 (in Chinese with English Abstract).

Brugger, J., Bettiol, A., Costa, S., Lahaye, Y., Bateman, R., Lambert, D., Jamieson, D., 2000. Mapping REE distribution in scheelite using luminescence. Mineral. Mag. 64, 891–903.

Brugger, J., Mass, R., Lahaye, Y., Mcrae, C., Ghaderi, M., Costa, S., Lambert, D., Bateman, R., Prince, K., 2002. Origins of Nd–Sr–Pb isotopic variations in single scheelite grains from Archaean gold deposits Western Australia. Chem. Geol. 182, 203–225.
Brugger, J., Etschmann, B., Pownceby, M., Liu, W., Grundler, P., Brewe, D., 2008. Oxidation state of europium in scheelite: tracking fluid-rock interaction in gold deposits. Chem. Geol. 257, 26–33.
Cai, M.H., Liang, T., Peng, Z.A., Fan, S.K., Luo, X.W., 2014. Geology and Metallogency of the Dachang Tin-polymetallic Orefield. Geological Publishing House, Beijing, pp. 1–143 (in Chinese with English abstract).
Cai, M.H., Peng, Z.N., Hu, Z.S., Li, Y., 2020. Zn, He-Ar and Sr-Nd isotopic compositions of the Tongkeng Tin-polymetallic ore deposit in south China: Implication for ore genesis. Ore Geol. Rev. 124, 103605.
Chen, Y.W., Bi, X.W., Fu, S.L., Dong, S.H., 2016. Zircon U-Pb dating and Hf isotope of the felsic dykes in the Longshan Au-Sb deposit in Central Hunan Province and their geological significance. Acta Petrol. Sin. 32, 3469–3488 (in Chinese with English abstract).
Dermatas, D., Braida, W., Christodoulatos, C., Strigul, N., Panikov, N., Los, M., Larson, S., 2004. Solubility, sorption, and soil respiration effects of tungsten and tungsten alloys. Environ. Forensic 5, 5–13.
Dill, H.G., Melcher, F., Botz, R., 2008. Meso- to epithermal W-bearing Sb vein-type deposits in calcareous rocks in western Thailand; with special reference to their metallogenetic position in SE Asia. Ore Geol. Rev. 34, 242–262.
Dolejs, D., Wagner, T., 2008. Thermodynamic modeling of non-ideal mineral–fluid equilibria in the system Si–Al–Fe–Mg–Ca–Na–K–H–O–Cl at elevated temperatures and pressures: Implications for hydrothermal mass transfer in granitic rocks. Geochim. Cosmochim. Acta 72, 526–553.
Dostal, J., Kontak, D.J., Chatterjee, A., 2009. Trace element geochemistry of scheelite and rutile from metaturbidite-hosted quartz vein gold deposits Meguma Terrane, Nova Scotia, Canada: genetic implications. Mineral. Petrol. 97, 95–109.
Du, Y.S., Huang, H.W., Huang, Z.Q., Xu, Y.J., Yang, J.H., Huang, H., 2009. Basin translation from Late Paleozoic to Triassic of Youjiang Basin and its tectonic significance. Geol. Sci. Technol. Inform. 28, 10–15 (in Chinese with English abstract).
Ewers, G.R., 1977. Experimental hot water-rock interactions and their significance to natural hydrothermal systems in New Zealand. Geochim. Cosmochim. Acta 41, 143–150.
Fan, D.L., Zhang, T., Ye, J., Pasava, J., Kribek, B., Dobes, P., Varrin, I., Zak, K., 2004. Geochemistry and origin of tin–polymetallic sulfide deposits hosted by the Devonian black shale series near Dachang, Guangxi, China. Ore Geol. Rev. 24, 103–120.
Faure, M., Shu, L.S., Wang, B., Charvet, J., Choulet, F., Monie, P., 2009. Intracontinental subduction: a possible mechanism for the Early Palaeozoic Orogen of SE China. Terra (Helsinki, Finland) 21, 360–368.
Fu, S.L., Hu, R.Z., Bi, X.W., Sullivan, N.A., Yan, J., 2020a. Trace element composition of stibnite: Substitution mechanism and implications for the genesis of Sb deposits in southern China. Appl. Geochem. 118, 104637.
Fu, S.L., Zajacz, Z., Tsay, A., Hu, R.Z., 2020b. Can magma degassing at depth donate the metal budget of large hydrothermal Sb deposits? Geochim. Cosmochim. Acta 290, 1–15.
Fu, S.L., Hu, R.Z., Yin, R.S., Yan, J., Mi, X.F., Song, Z.C., Sullivan, N.A., 2020c. Mercury and in situ sulfur isotopes as constraints on the metal and sulfur sources for the world's largest Sb deposit at Xikuangshan, Southern China. Miner. Deposita 55, 1353–1364.
Fu, Y., Hollings, P., Li, D.F., Liu, Q.F., Li, S.Y., Sun, X.M., 2021. Geochemistry of multi-stage scheelite in the skarn: Constraints on ore-forming processes of the Machangqing Cu-Mo polymetallic deposit in Yunnan Province, southwest China. Ore Geol. Rev. 138, 104370.
Fu, S.L., Wang, T.X., Yan, J., Pan, L.C., Wei, L.M., Lan, Q., 2022. Formation of the Banxi Sb deposit in Eastern Yangtze Block: evidence from individual fluid inclusion analyses, trace element chemistry, and He-Ar-S isotopes. Ore Geol. Rev. 146, 104949.
Fu, S.L., Hu, R.Z., Peng, J.T., Wu, L.Y., Ma, D.S., 2023. A comprehensive genetic model for the world's largest Sb deposit (Xikuangshan, China). Geol. Soc. Am. Bull. 35, 1074–1088.
Gao, L.Z., Dai, C.G., Liu, Y.X., Wang, M., Wang, X.H., Chen, J.S., Ding, X.Z., Zhang, C.H., Cao, Q., Liu, J.H., 2010. Zircon SHRIMP U-Pb dating of tuff bed of the Sibao Group in southeastern Guizhou-northern Guangxi area, China and its stratigraphic implication. Geol. Bull. China 29, 1259–1267 (in Chinese with English abstract).
Ghaderi, M., Palin, J.M., Campbell, I.H., Sylvester, P.J., 1999. Rare earth element systematics in scheelite from hydrothermal gold deposits in the Kalgoorlie-Norseman region, Western Australia. Econ. Geol. 94, 423–437.
Gunn, A.G. (Ed.), 2014. Critical Metals Handbook. Wiley, New York, pp. 1–439.
Guo, S., Chen, Y., Liu, C., Wang, J., Su, B., Gao, Y., Wu, F., Sein, K., Yang, Y., Mao, Q., 2016. Scheelite and coexisting F-rich zoned garnet, vesuvianite, fluorite, and apatite in calc-silicate rocks from the Mogok metamorphic belt, Myanmar: implications for metasomatism in marble and the role of halogens inWmobilization and mineralization. J. Asian Earth Sci. 117, 82–106.
Guo, J., Zhang, R.Q., Sun, W.D., Ling, M.X., Hu, Y.B., Wu, K., Luo, M., Zhang, L.C., 2018. Genesis of tin-dominant polymetallic deposits in the Dachang district, South China: insights from cassiterite U–Pb ages and trace element compositions. Ore Geol. Rev. 95, 863–879.
Han, F., Zhao, R.S., Shen, J.Z., Hutchinson, R.W., Jiang, S.Y., Chen, H.D., 1997. Geology and Origin of Ores in the Dachang Tin-polymetallic Ore Field. Geological Publishing House, Beijing, pp. 1–213.
Harlaux, M., Mercadier, J., Marignac, C., Peiffert, C., Cloquet, C., Cuney, M., 2018. Tracing metal sources in peribatholitic hydrothermal W deposits based on the chemical composition of wolframite: the example of the Variscan French Massif Central. Chem. Geol. 479, 58–85.
Hazarika, P., Mishra, B., Pruseth, K.L., 2016. Scheelite, apatite, calcite and tourmaline compositions from the late Archean Hutti orogenic gold deposit: implications for analogous two stage ore fluids. Ore Geol. Rev. 72, 989–1003.
He, J., Ma, D.S., Liu, Y.J., 1996. Geochemistry of mineralization in the Zhazixi antimony ore belt on the margin of the Jiangnan old land. Miner. Deposits 15, 41–51 (in Chinese with English abstract).
Henderson, P., 1985. Crystal chemistry and geochemistry of some mineral crystal. Geol. Geochem. Suppl. 1–4.
Hu, A.X., Peng, J.T., 2016. Mesozoic lamprophyre and its origin in the Xikuangshan district, central Hunan. Acta Petrol. Sin. 32, 2041–2056 (in Chinese with English abstract).
Hu, A.X., Peng, J.T., 2020. Characteristics and significance of the fluid inclusions from the Zhazixi Sb-W deposit, Hunan Province. Geotecton. Metallog. 44, 431–446 (in Chinese with English abstract).
Hu, R.Z., Zhou, M.F., 2012. Multiple Mesozoic mineralization events in South China-an introduction to the thematic issue. Miner. Deposita 47, 579–588.
Hu, R.Z., Fu, S.L., Huang, Y., Zhou, M.F., Zhao, C.H., Wang, Y.J., Bi, X.W., Xiao, J.F., 2017a. The giant South China Mesozoic low-temperature metallogenic domain: reviews and a new geodynamic model. J. Asian Earth Sci. 137, 9–34.
Hu, R.Z., Chen, W.T., Xu, D.R., Zhou, M.F., 2017b. Reviews and new metallogenic models of mineral deposits in South China: an introduction. J. Asian Earth Sci. 137, 1–8.
Irber, W., 1999. The lanthanide tetrad effect and its correlation with K/Rb, Eu/Eu*, Sr/Eu, Y/Ho, and Zr, Hf of evolving peraluminous granite suites. Geochim. Cosmochim. Acta 63, 489–508.
Jiang, S.Y., Han, F., Shen, J.Z., Palmer, M.R., 1999. Chemical and Rb-Sr, Sm-Nd isotopic systematics of tourmaline from the Dachang Sn-polymetallic ore deposit, Guangxi Province. P. R. China. Chem. Geol. 157, 49–67.
Kyono, A., Hayakawa, A., Horiki, M., 2015. Selenium substitution effect on crystal structure of stibnite (Sb2S3). Phys. Chem. Miner. 42, 475–490.
Lassner, E., Schubert, W.D., 1999. Tungsten Properties, Chemistry, Technology of the Elements, Alloys, and Chemical Compounds. New York. Kluwer Academic/Plenum Publishers, pp. 1–422.
Li, J.H., Zhang, Y.Q., Dong, S.W., Ma, Z.L., Li, Y., 2015. LA-MC-ICPMS zircon U-Pb geochronology of the Hongxiaqiao and Banshanpu granitoids in Eastern Hunan Province and its geological implications. Acta Geosci. Sin. 36, 187–196 (in Chinese with English abstract).
Li, X.Y., Gao, J.F., Zhang, R.Q., Lu, J.J., Chen, W.H., Wu, J.W., 2018a. Origin of the Muguayuan veinlet-disseminated tungsten deposit, South China Constraints from in situ trace element analyses of scheelite. Ore Geol. Rev. 99, 180–194.
Li, H., Wu, Q.H., Evans, N.J., Zhou, Z.K., Kong, H., Xi, X.S., Lin, Z.W., 2018b. Geochemistry and geochronology of the Banxi Sb deposit: Implications for fluid origin and the evolution of Sb mineralization in central-western Hunan, South China. Gondw. Res. 55, 112–134.
Li, H., Kong, H., Zhou, Z.K., Tindell, T., Tang, Y.Q., Wu, Q.H., Xi, X.S., 2019a. Genesis of the Banxi Sb deposit, South China: constraints from wall-rock geochemistry, fluid inclusion microthermometry, Rb–Sr geochronology, and H–O–S isotopes. Ore Geol. Rev. 115, 103162.
Li, J.D., Li, X.F., Xiao, R., 2019b. Multiple-stage tungsten mineralization in the Silurian Jiepai W skarn deposit, South China: insights from cathodoluminescence images, trace elements, and fluid inclusions of scheelite. J. Asian Earth Sci. 181, 103898.
Li, H., Zhu, D.P., Shen, L.W., Algeo, T.J., Elatikpo, S.M., 2022. A general ore formation model for metasediment-hosted Sb-(Au-W) mineralization of the Woxi and Banxi deposits in South China. Chem. Geol. 607, 121020.
Liang, T., 2008. Study on the Metallogenic Mechanism of Changpo-Tongkeng Tin-polymetallic Deposit, Dachang, Guangxi (A Dissertation Submitted to Chang'an University for Degree of Doctor of Philosophy. (in Chinese with English abstract)).
Liang, Y., Wang, G.G., Liu, S.Y., Sun, Y.Z., Huang, Y.G., Hoshino, K., 2014. A study on the mineralization of the Woxi Au–Sb–W deposit, Western Hunan, China. Resour. Geol. 65, 27–38.
Linnen, R.L., Williams-Jones, A.E., 1995. Genesis of a magmatic metamorphic hydrothermal system; the Sn-W polymetallic deposits at Pilok, Thailand. Econ. Geol. 90, 1148–1166.
Liu, B., Li, H., Wu, Q.H., Evans, N.J., Cao, Y.J., Jiang, J.B., Wu, J.H., 2019. Fluid evolution of Triassic and Jurassic W mineralization in the Xitian ore field, South China: constraints from scheelite geochemistry and microthermometry. Lithos 330, 1–15.
Long, Z.Y., Qiu, K.F., Santosh, M., Yu, H.C., Jiang, X.Y., Zou, L.Q., Tang, D.W., 2022. Fingerprinting the Metal Source and Cycling of the World's Largest Antimony Deposit in Xikuangshan. The Geological Society of America Bulletin, China. https://doi.org/10.1130/B36377.1.
Lu, X.W., Ma, D.S., Xie, Q.L., Wang, W.Y., 2001. Traceelement geochemical characteristics of Neoproterozoic–Paleozoic strata in western and central Hunan. Geology-Geochemistry 29, 24–30 (inChinese with English abstract).
Lu, Z.W., Li, S., Liu, D.Y., 2015. Metallogenic conditions and mechanism of Zhazixi symbiosis deposit of antimony and tungsten. Gold 36, 23–27 (in Chinese with English abstract).
Lu, Y.L., Peng, J.T., Yang, J.H., Hu, A.X., Li, Y.K., Tan, H.Y., Xiao, Q.Y., 2017. Petrogenesis of the Ziyunshan pluton in central Hunan, South China: constraints from zircon U-Pb dating, element geochemistry and Hf-O isotopes. Acta Petrol. Sin. 33, 1705–1728 (in Chinese with English abstract).
Ma, D.S., Pan, J.Y., Xie, Q.L., He, J., 2002. Ore source of Sb (Au) deposits in Central Hunan: I. Evidences of trace elements and experimental Geochemistry. Mineral Deposits 21, 366–376 (in Chinese with English abstract).

Mao, J.W., Cheng, Y.B., Chen, M.H., Pirajno, F., 2013. Major types and time-space distribution of Mesozoic ore deposits in South China and their geodynamic settings. Miner. Deposita 48, 267–294.
Nie, A.G., 1996. Research of ore-forming fluids of Chashan antimony deposit, Guangxi. J. Guizhou Inst. Technol. 25, 30–33 (in Chinese with English abstract).
Nie, A.G., 1998. REE geochemistry and origin of fluorites from Chashan antimony deposit, Guaingxi. Acta Mineral. Sin. 18, 250–253 (in Chinese with English abstract).
Peng, J.T., Zhang, D.L., Hu, R.Z., Wu, M.J., Lin, X.Y., 2008. Sm–Nd and Sr isotope geochemistry of hydrothermal scheelite from the Zhazixi W-Sb deposit, Western Hunan. Acta Geol. Sin. 82, 1514–1521 (in Chinese with English abstract).
Peng, J.T., Zhang, D.L., Hu, R.Z., Wu, M.J., Liu, X.M., Qi, L., Yu, Y.G., 2010. Inhomogeneous distribution of rare earth elements (REEs) in scheelite from the Zhazixi W-Sb deposit, western Hunan and its geological implications. Geol. Rev. 56, 810–819 (in Chinese with English abstract).
Phillips, G.N., Powell, R., 2010. Formation of gold deposits—a metamorphic devolatilization model. J. Metam. Geol. 28, 689–718.
Pi, Q.H., Hu, R.Z., Xiong, B., Li, Q.L., Zhong, R.C., 2017. In situ SIMS U-Pb dating of hydrothermal rutile: reliable age for the Zhesang Carlin-type gold deposit in the golden triangle region, SW China. Miner. Deposita 52, 1179–1190.
Pitcairn, I.K., Teagle, D.A.H., Craw, D., Olivo, G.R., Kerrich, R., Brewer, T.S., 2006. Sources of metals in orogenic gold deposits: Insights from the Otago and Alpine Schists, New Zealand. Econ. Geol. Bull. Soc. Econ. Geol. 101, 1525–1546.
Pitcairn, I.K., Olivo, G.R., Teagle, D.A.H., Craw, D., 2010. Sulfide evolution during prograde metamorphism of the Otago and Alpine schists, New Zealand. Can. Mineral. 48, 1267–1295.
Pitcairn, I.K., Skelton, A.D.L., Wohlgemuth-Ueberwasser, C.C., 2015. Mobility of gold during metamorphism of the Dalradian in Scotland. Lithos 233, 69–88.
Poulin, R.S., Kontak, D.J., McDonald, A., 2018. Assessing scheelite as an ore-deposit discriminator using its trace element and REE chemistry. Can. Mineral. 56, 265–302.
Raimbault, L., Baumer, A., Dubru, M., Benkerrou, C., Croze, V., Zahm, A., 1993. REE fractionation between scheelite and apatite in hydrothermal conditions. Am. Mineral. 78, 1275–1285.
Raju, P.V.S., Hart, C.J.R., Sangurmath, P., 2016. Scheelite geochemical signatures by LA-ICPMS and potential for rare earth elements from Hutti gold mines and fingerprinting ore deposits. J. Afr. Earth Sci. 114, 220–227.
Rempel, K.U., Williams-Jones, A.E., Migdisov, A.A., 2009. The partitioning of molybdenum (VI) between aqueous liquid and vapour at temperatures up to 370 °C. Geochim. Cosmochim. Acta 73 (11), 3381–3392.
Satish-Kumar, M., Hermann, J., Miyamoto, T., Osanai, Y., 2010. Fingerprinting a multistage metamorphic fluid-rock history: evidence from grain scale Sr, O and C isotopic and trace element variations in high-grade marbles from East Antarctica. Lithos 114, 217–228.
Schulz, K.J., DeYoung Jr., J.H., R, R.S.I., Bradley, D.C., 2017. Critical mineral resources of the United States—economic and environmental geology and prospects for future supply. U.S. Geol. Surv. Prof. Pap. 1802, 1–797.
Shen, N.P., Cai, J.L., Su, W.C., Dong, W.D., 2015. Characteristics and source significances of trace element geochemistry of fluorite from Chashan Sb-W deposit in Guangxi. Acta Geol. Sin. 89, 384–391 (in Chinese with English abstract).
Shi, C.Y., Yan, M.C., Chi, Q.H., 2007. Abundances of chemical elements of granitoids in different geotectonic units of China and their characteristics. Acta Geol. Sin. 81, 47–59 (in Chinese with English abstract).
Silyanov, S.A., Sazonov, A.M., Naumov, E.A., Lobastov, B.M., Zvyagina, Y.A., Artemyev, D.A., Nekrasova, N.A., Pirajno, F., 2022. Mineral paragenesis, formation stages and trace elements in sulfides of the Olympiada gold deposit (Yenisei Ridge, Russia). Ore Geol. Rev. 143, 104750.
Simons, B., Andersen, J.C.Ø., Shail, R.K., Jenner, F.E., 2017. Fractionation of Li, Be, Ga, Nb, Ta, In, Sn, Sb, W and Bi in the peraluminous Early Permian Variscan granites of the Cornubian Batholith: Precursor processes to magmatic-hydrothermal mineralization. Lithos 278-281, 491–512.
Song, G.X., Qin, K.Z., Li, G.M., Evans, N.J., Chen, L., 2014. Scheelite elemental and isotopic signatures: implications for the genesis of skarn-type W-Mo deposits in the Chizhou Area, Anhui Province, Eastern China. Am. Mineral. 99, 303–317.
Stergiou, C.L., Melfos, V., Voudouris, P., Papadopoulou, L., Spry, P.G., Peytcheva, I., Dimitrova, D., Stefanova, E., 2022. A fluid inclusion and critical/rare metal study of epithermal quartz-stibnite veins associated with the Gerakario porphyry deposit, Northern Greece. Appl. Sci. 12 (2), 909.
Sun, K.K., Chen, B., 2017. Trace elements and Sr-Nd isotopes of scheelite: implications for the W-Cu-Mo polymetallic mineralization of the Shimensi deposit, South China. Am. Mineral. 102, 1114–1128.
Sun, S.S., McDonough, W.F., 1989. Chemical and isotopic systematics of oceanic basalts: implication for mantle composition and processes. In: Saunder, A.D., Norry, M.J. (Eds.), Magmatism in the Ocean Basins. Geological Society, London, pp. 313–345. Special Publications 42.
Sun, K.K., Chen, B., Deng, J., 2019. Ore genesis of the Zhuxi supergiant W-Cu skarn polymetallic deposit, South China: evidence from scheelite geochemistry. Ore Geol. Rev. 107, 14–29.
Sylvester, P.J., Ghaderi, M., 1997. Trace element analysis of scheelite by excimer laser ablation inductively coupled plasma mass spectrometry (ELA-ICPMS) using a synthetic silicate glass standard. Chem. Geol. 141, 49–65.
Tang, Y.W., Han, J.J., Lan, T.G., Gao, J.F., Liu, L., Xiao, C.H., Yang, J.H., 2022. Two reliable calibration methods for accurate in-situ U-Pb dating of scheelite. J. Anal. At. Spectrom 37, 358–368.
Thomas, R., Förster, H.J., Rickers, K., Webster, J.D., 2005. Formation of extremely F-rich hydrous melt fractions and hydrothermal fluids during differentiation of highly evolved tin-granite magmas: a melt/fluid-inclusion study. In: Contribution to Mineralogy and Petrology, 148, pp. 582–601.
Wang, Y.L., Wang, D.H., 2022. Geology of Mineral Resource in China: Volume of Antimony Ore. Geological Publishing House, Beijing, pp. 1–890 (in Chinese).
Wang, Q., Zhao, Z.H., Jian, P., Xu, J.F., Bao, Z.W., Ma, J.L., 2004. SHRIMP zircon geochronology and Nd-Sr isotopic geochemistry of the Dexing granodiorite porphyries. Acta Petrol. Sin. 20, 315–324 (in Chinese with English abstract).
Wang, Y.L., Chen, Y.C., Wang, D.H., Xu, J., Chen, Z.H., 2012. Scheelite Sm-Nd dating of the Zhazixi W-Sb deposit in Hunan and its geological significance. Geol. China 39, 1339–1344 (in Chinese with English abstract).
Wang, J.Q., Shu, L.S., Santosh, M., 2016. Petrogenesis and tectonic evolution of Lianyunshan complex, South China: insights on Neoproterozoic and late Mesozoic tectonic evolution of the central Jiangnan Orogen. Gondw. Res. 39, 114–130.
Wang, T.Y., Li, G.J., Wang, Q.F., Santosh, M., Zhang, Q.Z., Deng, J., 2019. Petrogenesis and metallogenic implications of Late Cretaceous I- and S-type granites in Dachang–Kunlunguan ore belt, southwestern South China Block. Ore Geol. Rev. 113, 103079.
Webster, J., Thomas, R., Förster, H.J., Seltmann, R., Tappen, C., 2004. Geochemical evolution of halogen-enriched granite magmas and mineralizing fluids of the Zinnwald tin-tungsten mining district Erzgebirge, Germany. Miner. Deposita 39, 452–472.
Xiong, D.X., Sun, X.M., Shi, G.Y., Wang, S.W., Gao, J.F., Xue, T., 2006. Trace elements, rare earth elements (REE) and Nd-Sr isotopic compositions in scheelites and their implications for the mineralization in Daping gold mine in Yunnan province, China. Acta Petrol. Sin. 22, 733–741 (in Chinese with English abstract).
Yan, J., Fu, S.L., Liu, S., Wei, L.M., Wang, T.X., 2022. Giant Sb metallogenic belt in South China: a product of Late Mesozoic flat-slab subduction of paleo-Pacific plate. Ore Geol. Rev. 142, 104697.
Yuan, S.D., Williams-Jones, A.E., Mao, J.W., Zhao, P.L., Yan, C., Zhang, D.L., 2018. The origin of the Zhangjialong tungsten deposit, south China: implications for W-Sn mineralization in large granite batholiths. Econ. Geol. 113 (5), 1193–1208.
Yuan, S.D., Williams-Jones, A.E., Romer, R.L., Zhao, P.L., Mao, J.W., 2019. Protolith-related thermal controls on the decoupling of Sn and W in Sn-W metallogenic provinces: insights from the Nanling region, China. Econ. Geol. 114 (5), 1005–1012.
Zeng, G.P., Gong, Y.J., Hu, X.L., Xiong, S.F., 2017a. Geology, fluid inclusions, and geochemistry of the Zhazixi Sb–W deposit, Hunan, South China. Ore Geol. Rev. 91, 1025–1039.
Zeng, G.P., Gong, Y.J., Wang, Z.F., Hu, X.L., Xiong, S.F., 2017b. Structures of the Zhazixi Sb–W deposit, South China: implications for ore genesis and mineral exploration. J. Geochem. Explor. 182, 10–21.
Zhang, Y.X., Liu, Y.M., Gao, S.D., He, Q.G., 1990. Earth elements geochemical characteristics of tungstenic minerals: a distinguishing sign for ore-forming type. Geochimica 19, 11–20 (in Chinese with English abstract).
Zhang, J., Huang, W.T., Liang, T.Y., Wu, J., Chen, X.L., 2018. Genesis of the Jianzhupo Sb–Pb–Zn–Ag deposit and formation of an ore shoot in the Wuxu ore field, Guangxi, South China. Ore Geol. Rev. 102, 654–665.
Zhang, Z., Xie, G., Mao, J., Liu, W., Olin, P., Li, W., 2019. Sm-Nd dating and in-situ LAICP-MS trace element analyses of scheelite from the Longshan Sb-Au deposit, Xiangzhong metallogenic province, South China. Minerals 9 (2), 87.
Zhang, D.X., Pan, J.Q., Gao, J.F., Dai, T.G., Bayless, R.C., 2021. In situ LA ICP-MS analysis of trace elements in scheelite from the Xuefeng Uplift Belt, South China and its metallogenic implications. Ore Geol. Rev. 133, 104097.
Zhao, K.D., 2005. Isotope Geochemistry and Genetic Models of Two Types of Tin Deposits: Case Studies From the Dachang and the Furong Tin Deposits (A Dissertation Submitted to Nanjing University for Degree of Doctor of Philosophy).
Zhao, G.C., Cawood, P.A., 2012. Precambrian geology of China. Precambrian Res. 222–223, 13–54.
Zhao, K.D., Jiang, S.Y., Ni, P., Ling, H.F., Jiang, Y.H., 2007. Sulfur, lead and helium isotopic compositions of sulfide minerals from the Dachang Sn-polymetallic ore district in South China: implication for ore genesis. Mineral. Petrol. 89, 251–273.
Zhao, W.W., Zhou, M.F., Williams-Jones, A.E., Zhao, Z., 2018. Constraints on the uptake of REE by scheelite in the Baoshan tungsten skarn deposit, South China. Chem. Geol. 477, 123–136.
Zhao, K.D., Zhang, L.H., Palmer, M.R., Jiang, S.Y., Xu, C., Zhao, H.D., Chen, W., 2021. Chemical and boron isotopic compositions of tourmaline at the Dachang Sn-polymetallic ore district in South China: constraints on the origin and evolution of hydrothermal fluids. Miner. Deposita 56, 1589–1608.
Zhao, P.L., Chu, X., Williams-Jones, A.E., Mao, J.W., Yuan, S.D., 2022a. The role of phyllosilicate partial melting in segregating W and Sn deposits in W-Sn metallogenic provinces. Geology 50, 121–125.
Zhao, P.L., Yuan, S.D., Williams-Jones, A.E., Romer, R.L., Yan, C., Song, S.W., Mao, J.W., 2022b. Temporal separation of W and Sn mineralization by temperature-controlled incongruent melting of a single protolith: evidence from the Wangxianling area, Nanling region, South China. Econ. Geol. 117, 667–682.
Zhong, Y.F., Ma, C.Q., Yu, Z.B., Lin, G.C., Xu, H.J., Wang, R.J., Yang, K.G., Liu, Q., 2005. SHRIMP U-Pb zircon geochronology of the Jiuling granitic complex batholith in Jiangxi Province. Earth Sci. J. China Univ. Geosci. 30, 685–691.
Zhu, Y.N., Peng, J.T., 2015. Infrared microthermometric and noble gas isotope study of fluid inclusions in ore minerals at the Woxi orogenic Au–Sb–W deposit, western Hunan, South China. Ore Geol. Rev. 65, 55–69.
Zhu, J.J., Hu, R.Z., Richards, J.P., Bi, X.W., Stern, R., Lu, G., 2017. No genetic link between Late Cretaceous felsic dikes and Carlin-type Au deposits in the Youjiang basin, Southwest China. Ore Geol. Rev. 84, 328–337.
Zotov, A.V., Shikina, N.D., Akinfiev, N.N., 2003. Thermodynamic properties of the Sb (III) hydroxide complex $Sb(OH)_3$(aq) at hydrothermal conditions. Geochim. Cosmochim. Acta 67, 1821–1836.